Sources and migration characteristics of fluorine in the river water of a small karst watershed influenced by coal mining

Shuangxue Du, Li An, Jiangxun Huang, Qingguang Li*, Pan Wu and Xingqiang Guo

College of Resources and Environmental Engineering, Key Laboratory of Karst Georesources and Environment, Ministry of Education, Guizhou University, Guiyang, China

In high-fluorine geological background areas, the supergene geochemical process of fluorine has an impact on regional environmental health and safety, which has long been the focus of attention. However, in karst areas characterized by a high incidence of endemic fluorosis, the migration and transformation of fluorine in surface water have not received sufficient attention. This study investigated the joint influence of the weathering and erosion of carbonate rocks and coal-bearing strata on a typical small watershed. Accordingly, 239 samples representing 13 periods of hydrochemical samples were systematically collected to clarify the source, migration, and transformation characteristics of fluorine in surface water. The results revealed that the pH of the Huatan River was low in the rainy season and high in the dry season. The annual variation range of fluorine concentration was 0.11−0.40 mg/L. Although mining development produced acid mine drainage with high fluorine concentration, its impact at the watershed scale appeared to be limited. In terms of spatial scale, the concentration of fluorine in the Huatan River increased gradually from upstream to downstream. The dissolution of fluorite and other fluorine-bearing minerals had not reached the saturation state. The fluorine in the watershed primarily came from the dissolution of fluorine-bearing minerals, followed by the contribution of atmospheric precipitation. The release of fluorine adsorbed on the surface of clay minerals was not the main source of this element. The leaching of the watershed was shown to represent a critical transport process concerning fluorine in the Huatan River, and evaporation had a notable impact on the enrichment of fluorine in water.

KEYWORDS

fluorine-bearing minerals, leaching, evaporation, D-excess, acid mine drainage

1 Introduction

Fluoride, an essential trace element in the human body, is also an identified cause endemic environmental health events, such as dental fluorosis and bone fluorosis (Guo et al., 2021; Li et al., 2020; Wang et al., 2021; Balcerzak, 2022). The World Health Organization lists fluoride among the top ten chemicals of public health concern and indicates that the guideline limit for fluoride in drinking water should not exceed 1.5 mg/L (Aghapour et al., 2018; Wang et al., 2020). According to the Groundwater Quality Standard (GB14848-2017), Surface Water Environmental Quality Standard (GB3838-2002), and Living Drinking Water Sanitation Standard (GB 5749–2022), the content of fluoride in drinking water shall not exceed 1.0 mg/L (He et al., 2020; Cao et al., 2022; Hao et al., 2022). Globally, more than 200 million people are affected by drinking water containing fluoride levels exceeding these standards (Strunecka and Strunecky, 2020; Vithanage and Bhattacharya, 2015; Wang et al., 2020). In an aqueous environment, the primary forms of fluorine are F^-, HF, FeF^+, FeF_2^+, MnF^+, AlF_2^+, AlF^{2+}, $AlF_3(aq)$, AlF_4^-, MgF^+, CaF^+, NaF, and many other forms (Deng et al., 2011). Li X. et al. (2016) indicated that fluoride easily forms stable complex compounds with Al in acidic water. With increasing pH, the contents of NaF, MgF^+, and CaF^+ increase gradually, and weakly alkaline water bodies are dominated by ionic F^- (Li X. et al., 2016; Hao et al., 2022).

According to Fuge (2019) and Savenko and Savenko, (2020), the average fluorine concentration in unpolluted surface freshwaters worldwide is relatively low, ranging from < 0.05 to 1.6 mg/L, with a median of 0.1 mg/L. Fluoride in water has long been a matter of concern mainly because of the local health risks posed by excessive intake of fluoride. Scholarly attention to this issue has also mainly focused on the source and enrichment mechanism of fluoride in groundwater, along with health risk assessment (Ozsvath, 2009; Ghosh et al., 2013; Feng et al., 2020; Liu et al., 2021; Masood et al., 2022; Wu et al., 2022). Recent research has found high fluoride levels in groundwater widely distributed in the north, northeast, and northwest regions of China, mainly in shallow groundwater (He et al., 2020). In practical terms, the concentration of fluorine in water is affected by many factors, such as pH, dissolution and precipitation of fluorine-bearing minerals, the ion exchange process, evaporation, and so on. In alkaline water, HCO_3^- and OH^- are more likely to replace the adsorbed or isomorphic fluorine ions in clay, mica, and other fluorine-bearing minerals, resulting in increasing fluorine concentrations in surface water (Wenzel and Blum, 1992; Deng et al., 2011; Emenike et al., 2018).

Unfortunately, at the surface watershed scale, especially in terms of the high geological background area of fluorine in Southwest China, the migration and transformation process of fluorine in the surface water system has received inadequate

scholarly attention. The endemic fluorosis area, represented by the Bijie region in Southwest China, has a high soil fluoride content of 5,979 mg/kg (Wang et al., 2021). Furthermore, in the medium-to high-sulfur coal mining area of southwest China, the weathering of sulfide-rich coal-bearing strata can produce serious acid pollution in surface water (Zhang et al., 2021; Huang et al., 2022). The fluorine content in acid mine drainage (AMD) from the Zhijin mining area in Guizhou has been reported to be as high as 4.94 mg/L (Li X. et al., 2016). However, many factors are known to affect the geochemical process of fluorine in acidic water, and systematic research examining this topic remains scarce (Deng et al., 2011; Miguel et al., 2017). Therefore, the release of fluorine in the process of surface soil leaching may have a notable impact on the enrichment of fluorine in surface watershed water (Wenzel and Blum, 1992).

Thus, a typical small watershed in Jinsha County, Guizhou Province, which is controlled by the superposition of weathering and erosion of carbonate rocks and coal-bearing strata, was selected as the research object for this study. In the study area, we conducted a systematic collection and analysis of hydrochemical samples in different seasons in the watershed in order to reveal the temporal and spatial distribution characteristics of fluorine in the river water, as well as to clarify the sources, migration, and transformation characteristics in the process of surface water migration.

2 Materials and methods

2.1 Overview of the study area

The Huatan River is located at east longitude $106°29'10''$–$106°42'24''$and north latitude $27°20'43''$–$27°26'4''$, at an altitude of 760–1,095 m. This narrow and long watershed is a secondary water system in the middle and lower reaches of the Wujiang River.

The terrain is high in the southwest and low in the northeast. The river under consideration empties into the Pianyan River in the east. The drainage area is 321 km², the total length of the river is 59 km, the natural drop is 220m, the average gradient is 5.7‰, and the annual average runoff is 130 million m³. On the left bank of the river are three tributaries with catchment areas greater than 20 km². The Huatanhe Reservoir is located upstream of the study area and is an important local drinking water source. The Huatan River Watershed is characterized as the subtropical monsoon humid climate zone, featuring a mild climate, annual average rainfall of 1,057 mm, annual average temperature of 15.1°C, and annual average sunshine of 1,120.2 h. Due to the development of karst landforms, funnels, peaks, depressions, sinkholes, ambushes, and natural bridges are omnipresent.

The geotectonic position of the study area is located in the northeast structural deformation area of Bijie, Zunyi fault arch of

FIGURE 1
The regional geology and sampling point distribution of the Huatan River (Є$_{2-3}$ls: Cambrian Loushanguan group; P$_1$l: Permian Liangshan Formation; P$_1$m: Permian Maokou Formation; P$_2$l: Permian Longtan Formation; P$_2$c: Permian Changxing Formation; T$_1$y: Triassic Yelang formation; T$_1$yn: Triassic Yongningzhen formation).
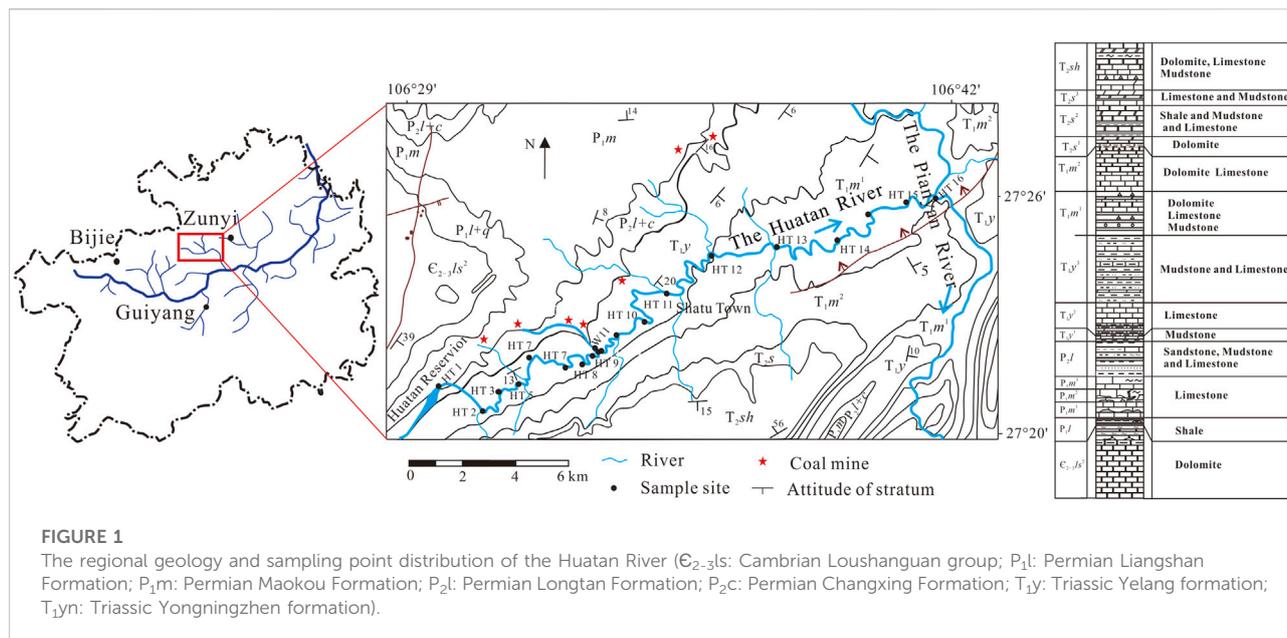
the Yangtze paraplatform, and Qianbei platform uplift. The structural features are mainly NE trending folds and fault zones, forming a barrier fold combination of wide and gentle anticlines and tight and narrow synclines. The area includes two groups of fault structures: NE trending and nearly EW trending.

The exposed strata in the study area include the lower Permian Maokou Formation (P$_1$m), the upper Longtan Formation (P$_2$l), the Changxing Formation (P$_2$c), and the lower Triassic Yelang Formation (T$_1$y). Lithologically, the strata mainly comprise carbonate rocks and clastic rocks. Carbonate rocks mainly include the Permian Qixia Formation (P$_1$q), Maokou Formation (P$_1$m), Changxing Formation (P$_2$c), Triassic Yelang Formation (T$_1$y), and Yongningzhen Formation (T$_1$yn). Specifically, the Longtan Formation is a coal-bearing rock series, with a thickness of about 95–110 m, containing 4–8 coal layers, and the coal is medium-sulfur anthracite. The Andi anticline is the primary coal controlling structure in the study area. The strata are monoclinal, and the occurrence is relatively stable. In the southeast wing of the anticline structure are many coal mines, such as the Huixin Coal Mine, the Yutiancheng Coal Mine, the Hongxing Coal Mine, the Hebian Coal Mine, and the Changsheng Coal Mine.

2.2 Sample collection and analysis

For the purposes of this study, we chose 18 sampling points in the Huatan River. One sampling point in the stream was affected by AMD (Figure 1). From August 2020 to November 2021, 13 time points of water samples were collected month by month. In addition, two groups of atmospheric precipitation

samples were collected in June and August 2021. During sampling, pH, water temperature (T/°C), conductivity (EC), and other variable parameters were recorded on site. The instrument used was the YSI Pro Plus multiparameter water-quality analyzer. Before sampling, the instrument electrodes were calibrated in advance. All samples collected were filtered through a 0.45 μm nylon membrane. Nitric acid was added to each subsample for cation analysis to adjust the pH < 2.0. Each subsample for anion analysis was filtered without reagent and stored in a 50 ml centrifuge tube. All samples were kept in the refrigerator at 4°C until analysis.

Anions, including F$^-$, Cl$^-$, NO$_3^-$, and SO$_4^{2-}$, were measured using the Dionex ICS-90 Ion Chromatography system (Dionex Corporation, Sunnyvale, CA, United States), while Ca^{2+}, Mg^{2+}, Na$^+$, K$^+$, and soluble SiO$_2$ were determined via the Vista MPX inductively coupled plasma optical emission spectrometer (ICP-OES; Varian, Inc., Palo Alto, CA, United States). Blank samples, parallel samples, and standard samples were added for quality control, and the charge conservation was controlled within ± 5%.

3 Results

The collected data revealed that the pH of the Huatan River was low in summer and autumn (rainy season) and high in winter and spring (dry season). The pH range was 7.47–8.96 (Table 1), and the average value was 8.19, which is generally weak alkaline. The pH in the stream (W11) affected by AMD was always acidic throughout the year, with a range of variation of 4.95–6.91 and an average of 6.43.

FIGURE 2
Variation characteristics of fluorine content along the Huatan River Basin.
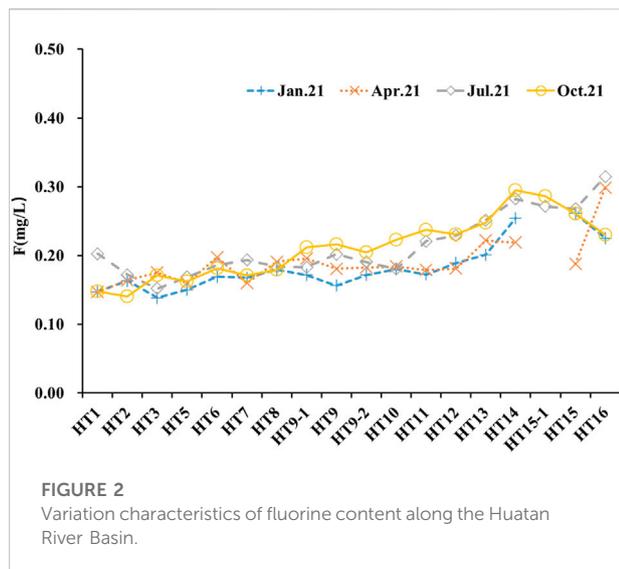
In terms of fluoride concentration, the annual variation range was 0.11–0.40 mg/L (Table 2), with an average of only 0.20 mg/L: Far lower than the limit of 1.0 mg/L for fluoride concentration in drinking water but higher than the average level of unpolluted rivers in the world. In the stream affected by AMD (W11), the concentration of fluorine varied from 0.45 to 1.54 mg/L, with an average of 1.05 mg/L, which was significantly higher than the concentration of fluorine in the Huatan River (Figure 2). In terms of spatial scale, the concentration of fluorine in the Huatan River Watershed demonstrated a gradually increasing trend from upstream to downstream. This finding may be explained by the location of mining activities in the basin, which are mainly in the middle and lower reaches. In terms of time scale, differences in fluorine concentration levels were not very obvious. According to the average level in the watershed, the rainy season was more than 0.20 mg/L, while the dry season was less than 0.20 mg/L.

4 Discussion

4.1 Relationship between fluorine content and hydrochemical parameters

Previous studies have shown that pH drives the form transformation of fluorine in water and is also an important factor affecting the adsorption and desorption of fluorine on the surface of clay minerals. According to Wenzel and Blum (1992), the solubility of fluorite is the smallest when the pH value is 6.0–6.5. Under acidic conditions, the hydroxyl groups on the surface of metal oxides and hydroxides (Al_2O_3, $Fe(OH)_2$) are easily replaced by ionic F^- (Li et al., 2015; Li et al., 2018). Meanwhile, under alkaline conditions, the adsorbed F^- on the surface of silicate minerals will be replaced by HCO_3^- and OH^-,

increasing the content of F^- in water (Parfitt and Russell, 1977; Bhatnagar et al., 2011; Mukherjee and Singh, 2020).

The current study findings revealed that the fluorine content in the AMD water samples significantly increased as pH decreased; in contrast, the fluorine content in the Huatan River water samples remained stable and did not increase as pH increased (Figure 3A). This observation indicates that the influence of pH on the resolution of adsorbed fluorine on the surface of silicate minerals in the watershed was limited. Theoretically, summer and autumn are rainy seasons with higher temperatures. Dilution from rainwater should result in a lower concentration of fluorine in river water than in dry seasons. However, as Figure 3 (b) shows, the concentration of fluorine in the Huatan River was higher in the rainy season than in the dry season. This observation may reflect the enhanced leaching and dissolution of fluorine-containing minerals in the rainy season. In addition, as can be seen in Figure 3, EC, SO_4^{2-}, HCO_3^-, Ca^{2+}, and soluble SiO_2 had no noteworthy correlation with fluorine. Obviously, the impact of these parameters in terms of fluoride levels in the river water was limited.

4.2 Hydrochemical composition of the huatan river

Hydrochemical composition of bodies of water often inherits the chemical composition characteristics of the bedrock in the source area (Gaillardet et al., 1999; Li Q. et al., 2016). Based on the ion ratio analysis of Na Standardization (Figure 4A), the hydrochemical composition of the river water in the Huatan River Watershed was primarily controlled by the dissolution of carbonate rocks and silicate rocks, and the influence of evaporates was weak. This finding is consistent with the geological background that carbonate rocks and coal-bearing rock series are widely distributed in the study area. According to the molar ratio of Mg/Ca and Na/Ca, the chemical composition of the river water in the Huatan River Watershed also demonstrated the common influence of dolomite and limestone (Figure 4B). Therefore, fluoride in carbonate rock and silicate rock may have been the dominant source of fluoride in the river water. Previous studies have also shown that carbonate-bound fluorine may be a predominant form of fluorine (Xu and Luo, 2008; Peng et al., 2021).

We sought to further reveal the impact of bedrock weathering and erosion on the chemical composition of river water in the watershed by mapping ion-equivalent concentrations of $Ca^{2+}+Mg^{2+}$ and $HCO_3^- + SO_4^{2-}$ and stoichiometric analysis. From the results presented in Figure 5A, it can be seen that most of the data points are located above the 1:1 evolution line, indicating that the dissolution of carbonate rocks and gypsum had a crucial impact on the chemical composition of the river water. Most of the data points are distributed above the evolution line, indicating the influence of additional HCO_3^- and SO_4^{2-} supplements. Meanwhile, in Figure 5B, after deducting the influence of the carbonate dissolution process

FIGURE 3
Correlation between fluorine content and different hydrochemical parameters in Huatan River Basin. (In all subgraphs, the cross symbol represents alkaline water, and the hollow triangle represents acidic water).
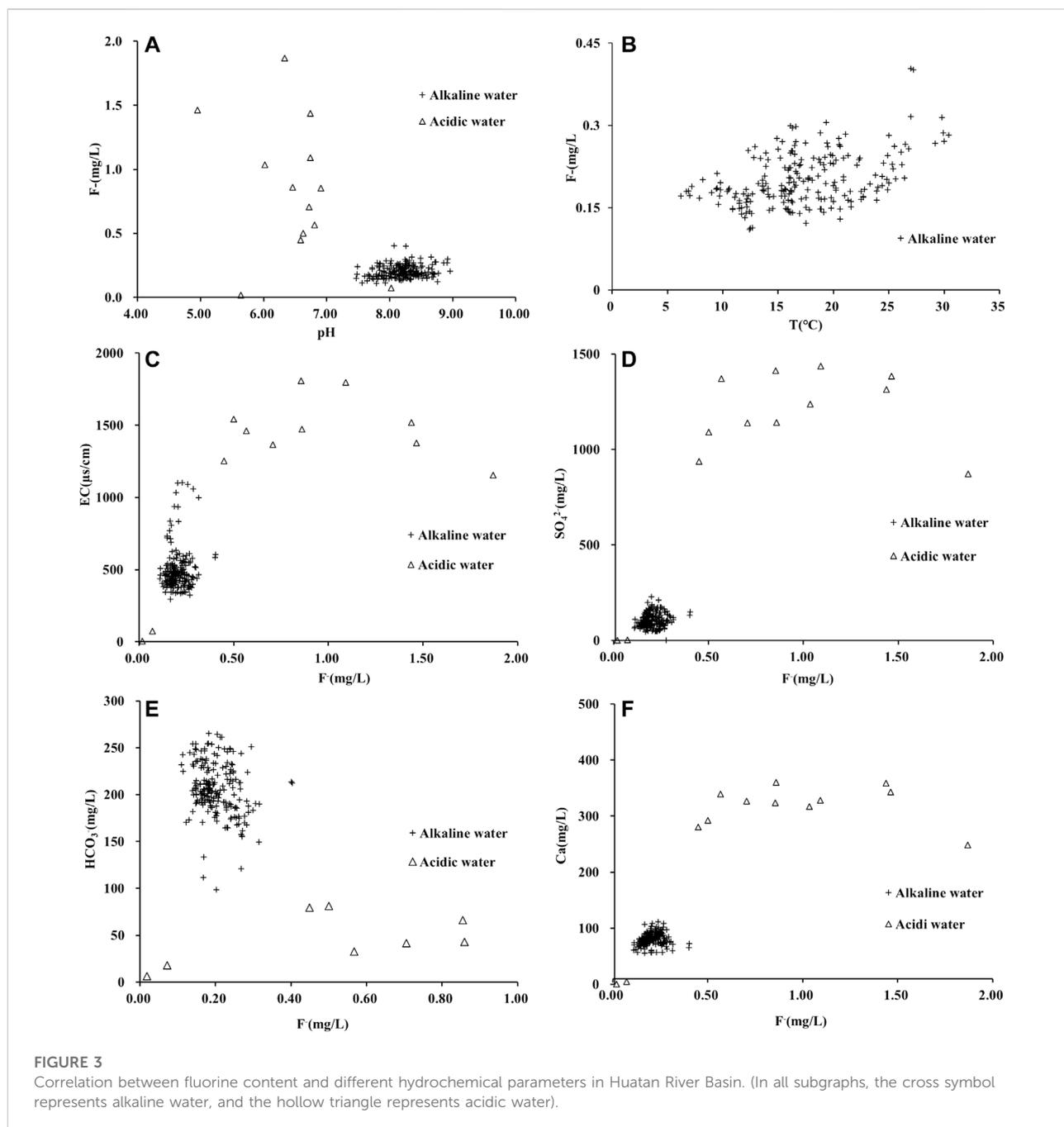
(Ca^{2+}+Mg^{2+}-0.5* HCO_3^-), most data points fall near the 1:1 evolution line, which further confirms that gypsum dissolution contributed a large quantity of SO_4^{2-} at the experimental site.

It is generally believed that Cl^- mainly comes from atmospheric precipitation and the dissolution of evaporates (Gaillardet et al., 1999; Zhong et al., 2017). Since the molar concentration ratio of Cl^- to Na^+ in atmospheric precipitation is close to 1:1, it can be derived from Figure 5C that the content of Na^+ in the Huatan River was much higher than that of Cl^-. Therefore, it is unlikely that Na^+ was mainly introduced

by from atmospheric precipitation. Considering that the contribution of evaporation was also minimal, Na^+ more likely resulted from the ion exchange process and the dissolution of silicate minerals such as clay. The problem is that the dissolved SiO_2 component in Figure 5D seems to have exerted a limited impact on fluorine in the Huatan River. Therefore, even if an extensive dissolution process of silicate minerals was occurring in the watershed, the release of adsorbed fluorine from clay minerals was not the principal source of fluorine in the Huatan River.

FIGURE 4
Identification of chemical sources in the Chetian River based on **(A)** HCO_3^-/Na^+ versus Ca^{2+}/Na^+ and **(B)** Mg^{2+}/Ca^{2+} versus Na^+/Ca^{2+}.

FIGURE 5
Recognition of the contribution of minerals' dissolution to water chemical composition based on scatterplots of **(A)** $Ca^{2+}+Mg^{2+}$ versus $HCO_3^- + SO_4^{2-}$; **(B)** $(Ca^{2+}+Mg^{2+})-0.5*HCO_3^-$ versus SO_4^{2-}; **(C)** Na^+ versus Cl^-; **(D)** F^- versus SiO_2.

FIGURE 6
(A) Relationship between Cl^- and F^-; **(B)** F^-/Cl^- versus F^- in the Huatan River.

FIGURE 7
Plots of **(A)** CAI-1 versus CAI-2 used to describe cation exchange; **(B)** calcite saturation index versus fluorite saturation index; **(C)** fluorite saturation index versus gypsum saturation index; **(D)** fluorite concentration versus fluorite saturation index.

4.3 Sources of fluorine in the huatan river

Cl^- and F^- are halogens with very similar chemical properties. As illustrated in Figure 6A, a certain correlation existed between Cl^- and F^- in the river water of the Huatan River Watershed. The two rainwater samples collected in June and August 2021 revealed concentrations of fluorine of 0.02 mg/L and 0.07 mg/L, respectively; meanwhile, the concentration of fluorine in the

FIGURE 8
Gibbs diagram of the Huatan River based on the relationship of **(A)** TDS versus $Na^+/(Na^++Ca^{2+})$; **(B)** TDS versus $Cl^-/(Cl^-+HCO_3^-)$.
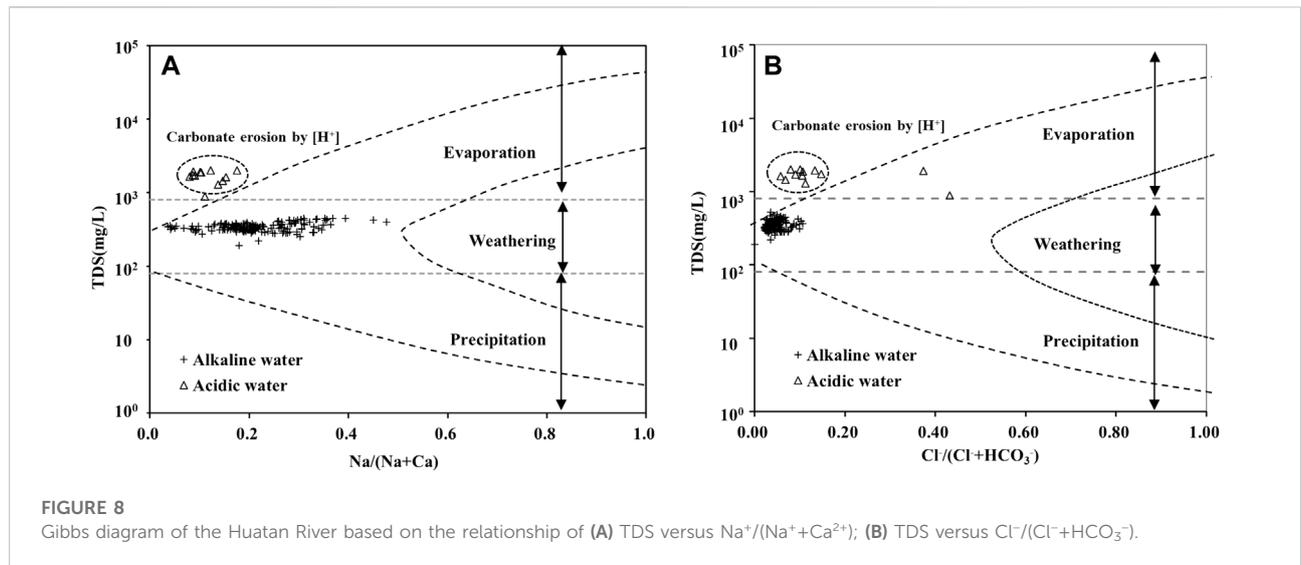
TABLE 1 pH data of river water in different months in the Huatan River Basin.

Date position	20.08	20.11	20.12	21.01	21.03	21.04	21.05	21.06	21.07	21.08	21.09	21.10	21.11
HT1	8.13	7.83	8.14	8.28	8.76	8.59	8.58	7.68	8.96	7.48	7.64	7.47	7.79
HT2	7.55	7.94	8.03	7.99	8.11	8.38	8.15	7.60	7.83	7.79	7.81	7.74	7.56
HT3	7.86	8.09	8.27	8.33	8.34	8.46	8.15	7.72	8.03	7.88	7.95	7.87	7.93
HT5	7.98	8.32	8.46	8.59	8.49	8.67	7.80	7.68	7.90	7.66	8.08	8.09	8.21
HT6	7.92	8.24	8.26	8.53	8.45	8.61	8.16	7.74	8.01	7.72	7.99	8.09	7.90
HT7	7.93	8.30	8.40	8.44	8.39	8.69	8.34	7.90	8.22	7.96	8.18	8.16	8.16
HT8	7.88	8.35	8.41	8.41	8.32	8.68	8.37	7.78	8.21	7.49	8.20	8.19	8.16
HT9-1		8.41	8.43	8.54	8.38	8.56	8.52	7.84	8.26	8.10	8.25	8.14	8.18
HT9	7.53	8.05	8.16	8.26	8.20	8.61	8.41	7.66	8.08	7.92	8.02	8.00	7.91
HT9-2		8.22	8.27	8.32	8.31	8.71	8.43	7.99	8.21	7.89	8.22	8.20	8.16
HT10	8.13	8.33	8.34	8.41	8.38	8.70	8.41	8.08	8.27	7.91	8.25	8.20	8.22
HT11	7.92	8.37	8.40	8.46	8.34	8.37	8.49	8.07	8.17	7.83	8.25	8.21	8.30
HT12	7.95	8.39	8.41	8.51	8.32	8.50	8.52	8.06	8.23	7.84	8.26	8.23	8.25
HT13	8.04	8.27	8.34	8.42	8.19	8.43	8.17	8.06	8.24	7.85	8.16	8.02	8.09
HT14	8.22	8.29	8.39	8.36	8.62	8.67	8.20	8.14	8.27	7.94	8.30	8.24	8.30
HT15-1									8.29	7.80	8.01	8.02	8.11
HT15	8.24		8.15	8.24	8.68	8.77	8.72	8.31	8.38	8.16	8.07	7.85	7.90
HT16	8.32	8.12	8.11	8.24	8.73	8.92	8.49	8.35	8.66	8.26	8.26	7.72	7.90
W11	6.17	6.81	6.74	6.91	6.58	6.74	6.72	6.02	6.46	4.95	6.33	6.59	6.63
AVE.	7.97	8.22	8.29	8.37	8.41	8.61	8.35	7.92	8.23	7.86	8.11	8.02	8.06

Huatan River varied from 0.11 to 0.40 mg/L, with an average of 0.20 mg/L. Therefore, although atmospheric deposition should have contributed a certain amount of exogenous fluorine to the Huatan River, it was not the river's main source of fluorine. Prior research has shown that during the process of evaporation, the molar concentrations of Cl^- and F^- increase in the same proportion; in contrast, the process of dissolution of fluorine-bearing minerals results in an increased concentration of F^-, while the concentration

TABLE 2 Data of fluorine concentration in different months in Huatan River Basin (mg/L).

Date position	20.08	20.11	20.12	21.01	21.03	21.04	21.05	21.06	21.07	21.08	21.09	21.10	21.11
HT1	0.19	0.17	0.18	0.15	0.12	0.15	0.17	0.17	0.20	0.18	0.13	0.15	0.11
HT2	0.11	0.17	0.16	0.16	0.15	0.16	0.14	0.17	0.17	0.18	0.14	0.14	0.11
HT3	0.20	0.15	0.18	0.14	0.14	0.18	0.17	0.15	0.15	0.16	0.15	0.17	0.11
HT5	0.12	0.15	0.16	0.15	0.14	0.16	0.27	0.15	0.17	0.18	0.15	0.16	0.14
HT6	0.17	0.17	0.15	0.17	0.19	0.20	0.18	0.16	0.19	0.22	0.15	0.18	0.14
HT7	0.15	0.18	0.18	0.17	0.24	0.16	0.20	0.17	0.19	0.23	0.19	0.17	0.15
HT8	0.08	0.19	0.18	0.18	0.25	0.19	0.22	0.16	0.18	0.24	0.20	0.18	0.14
HT9-1		0.18	0.18	0.17	0.24	0.20	0.15	0.21	0.18	0.23	0.16	0.21	0.13
HT9	0.16	0.19	0.18	0.16	0.20	0.18	0.16	0.16	0.20	0.19	0.18	0.22	0.15
HT9-2		0.19	0.19	0.17	0.25	0.18	0.21	0.19	0.19	0.25	0.21	0.20	0.17
HT10	0.23	0.21	0.20	0.18	0.20	0.18	0.24	0.21	0.18	0.25	0.20	0.22	0.17
HT11	0.10	0.20	0.18	0.17	0.22	0.18	0.27	0.20	0.22	0.24	0.23	0.24	0.17
HT12	0.18	0.18	0.18	0.19	0.30	0.18	0.24	0.19	0.23	0.27	0.24	0.23	0.16
HT13	0.15	0.24	0.21	0.20	0.23	0.22	0.23	0.23	0.25	0.26	0.24	0.25	0.18
HT14	0.23	0.25	0.24	0.25	0.23	0.22	0.25	0.26	0.28	0.28	0.25	0.30	0.19
HT15-1									0.27	0.25	0.27	0.29	0.20
HT15	0.15		0.24	0.26	0.26	0.19	0.28	0.29	0.27	0.26	0.40	0.26	0.20
HT16	0.22	0.26	0.25	0.23	0.28	0.30	0.31	0.32	0.31	0.28	0.40	0.23	0.20
W11	1.26	0.57	1.09	0.86	1.54	1.44	0.71	1.03	0.86	1.46	1.87	0.45	0.50
AVE.	0.16	0.19	0.19	0.18	0.21	0.19	0.22	0.20	0.21	0.23	0.22	0.21	0.16

FIGURE 9
(A) Plot of F⁻ concentration versus $\delta^{18}O$; (B) Plot of F⁻ concentration versus D-excess.
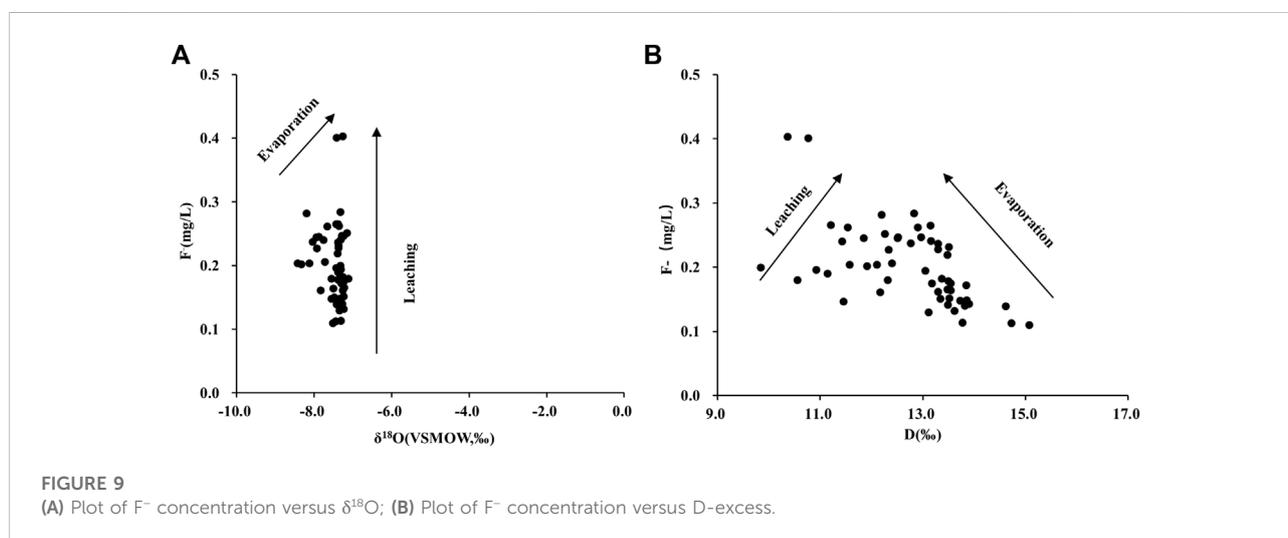
of Cl⁻ remains stable (Olaka et al., 2016). In light of those previous findings, evaporation was not the main process that induced an increase in fluorine concentration in the surface water in the watershed under consideration. Therefore, the fluorine in the Huatan River may be mainly attributed to the dissolution of fluorine minerals in the watershed (Figure 6B).

4.4 Dissolution and ion exchange of fluorine-bearing minerals

To date, the known fluorine-bearing minerals include fluorite (CaF_2), fluorapatite ($Ca_5(PO_4)_3F$), magnesium fluoride (MgF_2), aluminophosphate ($AlPO_4(F, OH)$), and

others, totaling more than 80 kinds (Deng et al., 2011; Barathi et al., 2019). Under alkaline conditions, the supersaturated state of calcite, dolomite, and other carbonate minerals will promote the reduction of Ca^{2+} and Mg^{2+} concentration and accelerate the dissolution of fluorite, fluorapatite, and other fluorine-bearing minerals, leading to increasing F^- concentration [Eqs. 1–3] (Chen et al., 2020; Zhang et al., 2021; Hao et al., 2022).

$$CaF_2 + 2HCO_3^- \rightarrow CaCO_3 + 2F^- + H_2O + CO_2 \quad (1)$$

$$CaF_2 + H_2O + CO_2\,(g) \rightarrow CaCO_3 + 2F^- + 2H^+ \quad (2)$$

$$Ca_5\,(PO_4)_3F + OH^- \rightarrow Ca_5\,(PO_4)_3OH + F^- \quad (3)$$

$$CaF_2 + SO_4^{2-} + 2H_2O \rightarrow CaSO_4 \bullet 2H_2O + 2F^- \quad (4)$$
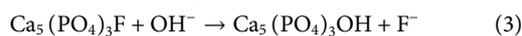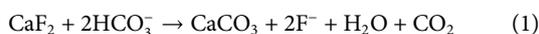
The results of the saturation index show that the dissolution of fluorite in the Huatan River Watershed had not reached a saturation state (Figure 7). Calcite revealed supersaturation, which obviously accelerated the dissolution of fluorite, fluorapatite, and other fluorine-bearing minerals. Furthermore, as F^- concentration increased, the saturation index of fluorite demonstrated the law of synchronous increase. Consequently, the dissolution of fluorite can be deemed a vital source of fluorine in the watershed.

In addition, according to Eq. 4, high concentrations of SO_4^{2-} can promote the dissolution of fluorite (Shao et al., 2021; Hao et al., 2022). In the Huatan River Watershed, gypsum also demonstrated an unsaturated state. Mining development in the study area caused the oxidation of a large number of sulfides and transported a large amount of SO_4^{2-} into the Huatan River, which obviously further promoted the dissolution of fluorite.

The chloro-alkaline index (CAI-1 and CAI-2) can be used to estimate the exchange process between main cations in water (Magesh et al., 2020; Hao et al., 2022). When CAI-1 and CAI-2 are less than 0, Ca^{2+} and Mg^{2+} in water tend to exchange with Na^+ and K^+ in silicate minerals. When both CAI-1 and CAI-2 are > 0, Na^+ and K^+ in water tend to exchange with Ca^{2+} and Mg^{2+} in carbonate minerals. Thus, Figure 7A reveals an obvious trend in terms of Ca^{2+} and Mg^{2+} in water replacing Na^+ and K^+ in silicate minerals in the Huatan River Watershed. This conclusion is observably consistent with the view in Figure 5C. Hence, this process can be considered conducive to the release of adsorbed F^- from silicate minerals.

4.5 Evaporation and leaching in the huatan river watershed

A Gibbs diagram is useful for describing the three processes that control changes in water chemical composition: Evaporation, atmospheric rainfall, and water–rock interactions (Li et al., 2015; Li Q. et al., 2016). A perusal of Figure 8A reveals that the impact of atmospheric precipitation and evaporation on the hydrochemical composition of the Huatan River Watershed is minimal. Under the condition where TDS remains basically unchanged, the Na/(Na +

Ca) ratio maintains a wide variation range, simply reflecting the process of Ca^{2+} and Mg^{2+} replacing Na^+ and K^+ in silicate minerals, as shown in Figure 7A, in which $Cl^-/(Cl^-+HCO_3^-)$ remains stable.

Evaporation is a notable means of oxygen isotope fractionation in surface water. When strong evaporation is taking place, the oxygen isotope composition becomes heavier, and the F^- concentration in the water body also increases synchronously. At the same time, in the process of evaporation, because the enrichment of ^{18}O is higher than that of D, the D excess will be less than 10‰ (Chen et al., 2021; Mandal et al., 2021; Pant et al., 2021). In addition, during the leaching process, the concentration of F^- increased; however, the variation of $\delta^{18}O$ was limited.

In order to further reveal the influence of evaporation and leaching on F^- enrichment in the watershed, we analyzed the hydrogen and oxygen isotopic composition of water samples in August, September, and November 2021. Figure 9 illustrates the evaporation and leaching processes. As can be observed from the figure, both evaporation and the leaching process had a certain impact on the enrichment of F^- in the watershed; moreover, the impact of the leaching process was more obvious. This conclusion is consistent with the F^-–Cl^- molar ratio (Figure 6B) and Gibbs diagram (Figure 7).

5 Conclusion

The annual variation range of fluorine concentration in the Huatan River Watershed is 0.11–0.40 mg/L, with an average of 0.20 mg/L. In terms of seasonal variation characteristics, the fluorine concentration was higher in the rainy season than in the dry season. The fluorine concentration in the Huatan River also showed spatial variation, increasing gradually along the flow direction; that said, the impact of AMD input on fluorine concentration in the watershed was limited. The water chemical composition of the Huatan River Watershed was generally controlled by the dissolution of carbonate and silicate rocks, and the influence of evaporation was weak. Lastly, the Huatan River Watershed revealed an obvious process where Ca^{2+} and Mg^{2+} was replacing Na^+ and K^+ in silicate minerals.

The dissolution of fluorite and other fluorine-bearing minerals was determined to be a major source of fluorine in the watershed water. Meanwhile, atmospheric precipitation contributed an observable share of fluorine to the Huatan River Watershed. According to the results of the saturation index calculation, the dissolution of fluorite in the Huatan River Watershed was not saturated, and calcite was in a supersaturated state, which was conducive to the dissolution of fluorite, fluorapatite, and other fluorine-bearing minerals. Thus, albeit both evaporation and the leaching process had an evident impact on the enrichment of F^- in the watershed, the influence of the watershed scale leaching process was more obvious.

Data availability statement

The raw data supporting the conclusions of this article will be made available by the authors, without undue reservation.

Author contributions

DS Writing-original draft Data curation Formal analysis Investigation LQ Conceptualization Funding acquisition Writing-review and; editing Data curation Formal analysis Investigation AL Conceptualization Writing-review and; editing Formal analysis Resources HJ Conceptualization Formal analysis WP Supervision Conceptualization Formal analysis GX Investigation Formal analysis.

Funding

Conflict of interest

The authors declare that the research was conducted in the absence of any commercial or financial relationships that could be construed as a potential conflict of interest.

Publisher's note

All claims expressed in this article are solely those of the authors and do not necessarily represent those of their affiliated organizations, or those of the publisher, the editors and the reviewers. Any product that may be evaluated in this article, or claim that may be made by its manufacturer, is not guaranteed or endorsed by the publisher.

References

Aghapour, S., Bina, B., Tarrahi, M. J., Amiri, F., and Ebrahimi, A. (2018). Distribution and health risk assessment of natural fluoride of drinking groundwater resources of Isfahan, Iran, using GIS. *Environ. Monit. Assess.* 190 (3), 137. doi:10.1007/s10661-018-6467-z

Balcerzak, M. (2022). "Biomonitoring of human exposure to fluorine," in *Handbook of bioanalytics* (Cham: Springer International Publishing), 1–18.

Barathi, M., Kumar, A. S. K., and Rajesh, N. (2019). Impact of fluoride in potable water–An outlook on the existing defluoridation strategies and the road ahead. *Coord. Chem. Rev.*, 387, 121–128. doi.org/doi:10.1016/j.ccr.2019.02.006

Bhatnagar, A., Kumar, E., and Sillanpää, M. (2011). Fluoride removal from water by adsorption—A review. *Chem. Eng. J.*, 171(3), 811–840. doi.org/doi:10.1016/j.cej.2011.05.028

Cao, H., Xie, X., Wang, Y., and Liu, H. (2022). Predicting geogenic groundwater fluoride contamination throughout China. *J. Environ. Sci.*, 115, 140–148. doi.org/doi:10.1016/j.jes.2021.07.005

Chen, Q., Dong, F., Jia, Z., Wei, J., Jia, C., An, M., et al. (2020). The experimental study of fluorine-leaching ability of granite with different solutions: A new insight into the dynamic of groundwater fluorine levels along coastal zones. *J. Contam. Hydrology*, 235, 103703. doi.org/doi:10.1016/j.jconhyd.2020.103703

Chen, X., Jiang, C., Zheng, L., Zhang, L., Fu, X., Chen, S., et al. (2021). Evaluating the Genesis and dominant processes of groundwater salinization by using hydrochemistry and multiple isotopes in a mining city. *Environ. Pollut.* 283, 117381. doi:10.1016/j.envpol.2021.117381

Deng, Y., Nordstrom, D. K., and McCleskey, R. B. (2011). Fluoride geochemistry of thermal waters in yellowstone national park: I. Aqueous fluoride speciation. *Geochimica Cosmochimica Acta*, 75(16), 4476–4489. doi:10.1016/j.gca.2011.05.028

Emenike, C. P., Tenebe, I. T., and Jarvis, P. (2018). Fluoride contamination in groundwater sources in Southwestern Nigeria: Assessment using multivariate statistical approach and human health risk. *Ecotoxicol. Environ. Saf.*, 156, 391–402. doi.org/doi:10.1016/j.ecoenv.2018.03.022

Feng, F., Jia, Y., Yang, Y., Huan, H., Lian, X., Xu, X., et al. (2020). Hydrogeochemical and statistical analysis of high fluoride groundwater in northern China. *Environ. Sci. Pollut. Res.* 27 (28), 34840–34861. doi:10.1007/s11356-020-09784-z

Fuge, R. (2019). Fluorine in the environment, a review of its sources and geochemistry. *Appl. Geochem.* 100, 393–406. doi:10.1016/j.apgeochem.2018.12.016

Gaillardet, J., Dupré, B., Louvat, P., and Allegre, C. J. (1999). Global silicate weathering and CO2 consumption rates deduced from the chemistry of large rivers. *Chem. Geol.*, 159(1-4), 3–30. doi.org/doi:10.1016/S0009-2541(99)00031-5

Ghosh, A., Mukherjee, K., Ghosh, S. K., and Saha, B. (2013). Sources and toxicity of fluoride in the environment. *Res. Chem. Intermed.* 39 (7), 2881–2915. doi:10.1007/s11164-012-0841-1

Guo, J., Wu, H., Zhao, Z., Wang, J., and Liao, H. (2021). Review on health impacts from domestic coal burning: Emphasis on endemic fluorosis in Guizhou Province, southwest China. *Rev. Environ. Contam. Toxicol.* 258, 1–25. doi:10.1007/398_2021_71

Hao, C., Sun, X., Xie, B., and Hou, S. (2022). Increase in fluoride concentration in mine water in Shendong mining area, Northwest China: Insights from isotopic and geochemical signatures. *Ecotoxicol. Environ. Saf.* 236, 113496. doi:10.1016/j.ecoenv.2022.113496

He, X., Li, P., Ji, Y., Wang, Y., Su, Z., Elumalai, V., et al. (2020). Groundwater arsenic and fluoride and associated arsenicosis and fluorosis in China: Occurrence, distribution and management. *Expo. Health* 12 (3), 355–368. doi:10.1007/s12403-020-00347-8

Huang, J., Li, Q., Wu, Pan., Wang, S., Guo, M., and Liu, K. (2022). The effects of weathering of coal-bearing stratum on the transport and transformation of DIC in karst watershed. *Sci. Total Environ.* 838, 156436. doi:10.1016/j.scitotenv.2022.156436

Li, C., Gao, X., and Wang, Y. (2015). Hydrogeochemistry of high-fluoride groundwater at Yuncheng Basin, northern China. *Sci. Total Environ.*, 508, 155–165. doi.org/doi:10.1016/j.scitotenv.2014.11.045

Li, D., Gao, X., Wang, Y., and Luo, W. (2018). Diverse mechanisms drive fluoride enrichment in groundwater in two neighboring sites in northern China. *Environ. Pollut.*, 237, 430–441. doi.org/doi:10.1016/j.envpol.2018.02.072

Li, M., Qu, X., Miao, H., Wen, S., Hua, Z., Ma, Z., et al. (2020). Spatial distribution of endemic fluorosis caused by drinking water in a high-fluorine area in Ningxia, China. *Environ. Sci. Pollut. Res.* 27 (16), 20281–20291. doi:10.1007/s11356-020-08451-7

Li, Q., Ju, Y., Lu, W., Wang, G., Neupane, B., Sun, Y., et al. (2016b). Water-rock interaction and methanogenesis in formation water in the southeast Huaibei coalfield, China. *Mar. Petroleum Geol.*, 77, 435–447. doi.org/doi:10.1016/j.marpetgeo.2016.06.021

Li, X., Wu, P., Han, Z., and Shi, J. (2016a). Sources, distributions of fluoride in waters and its influencing factors from an endemic fluorosis region in central Guizhou, China. *Environ. Earth Sci.* 75 (11), 981. doi:10.1007/s12665-016-5779-y

Liu, J., Peng, Y., Li, C., Gao, Z., and Chen, S. (2021). A characterization of groundwater fluoride, influencing factors and risk to human health in the southwest plain of Shandong Province, North China. *Ecotoxicol. Environ. Saf.*, 207, 111512. doi.org/doi:10.1016/j.ecoenv.2020.111512

Magesh, N. S., Botsa, S. M., Dessai, S., Mestry, M., Leitao, T. D. L., Tiwari, A., et al. (2020). Hydrogeochemistry of the deglaciated lacustrine systems in Antarctica: Potential impact of marine aerosols and rock-water interactions. *Sci. Total Environ.*, 706, 135822. doi.org/doi:10.1016/j.scitotenv.2019.135822

Mandal, R., Das, A., Sudheer, A. K., Kumar, S., Verma, S., Gaddam, M., et al. (2021). Sources, controls, and probabilistic health risk assessment of fluoride contamination in groundwater from a semi-arid region in Gujarat, Western India: An isotope–hydrogeochemical perspective. *Environ. Geochem. Health* 43 (10), 4043–4059. doi.org/10.1007/s10653-021-00894-2

Masood, N., Hudson-Edwards, K. A., and Farooqi, A. (2022). Groundwater nitrate and fluoride profiles, sources and health risk assessment in the coal mining areas of Salt Range, Punjab Pakistan. *Environ. Geochem. Health* 44 (3), 715–728. doi:10.1007/s10653-021-00987-y

Miguel, M. G., Barreto, R. P., and Pereira, S. Y. (2017). Study of a tropical soil in order to use it to retain aluminum, iron, manganese and fluoride from acid mine drainage. *J. Environ. Manag.* 204, 563–570. doi:10.1016/j.jenvman.2017.09.024

Mukherjee, I., and Singh, U. K. (2020). Fluoride abundance and their release mechanisms in groundwater along with associated human health risks in a geologically heterogeneous semi-arid region of east India. *Microchem. J.*, 152, 104304. doi.org/doi:10.1016/j.microc.2019.104304

Olaka, L. A., Wilke, F. D., Olago, D. O., Odada, E. O., Mulch, A., Musolff, A., et al. (2016). Groundwater fluoride enrichment in an active rift setting: Central Kenya rift case study. *Sci. Total Environ.* 545, 641–653. doi:10.1016/j.scitotenv.2015.11.161

Ozsvath, D. L. (2009). Fluoride and environmental health: A review. *Rev. Environ. Sci. Biotechnol.* 8 (1), 59–79. doi:10.1007/s11157-008-9136-9

Pant, N., Rai, S. P., Singh, R., Kumar, S., Saini, R. K., Purushothaman, P., et al. (2021). Impact of geology and anthropogenic activities over the water quality with emphasis on fluoride in water scarce Lalitpur district of Bundelkhand region, India. *Chemosphere*, 279, 130496. doi.org/doi:10.1016/j.chemosphere.2021.130496

Parfitt, R. L., and Russell, J. D. (1977). Adsorption on hydrous oxides. IV. Mechanisms of adsorption of various ions on goethite. *J. Soil Sci.*, 28(2), 297–305. doi.org/10.1111/j.1365-2389.1977.tb02238.x

Peng, B., Li, X., Ma, Z., and Qi, Y. (2021). Release of fluorine and chlorine during increase of phosphate rock grade by calcination and digestion. *Environ. Pollut.*, 270, 116321. doi.org/doi:10.1016/j.envpol.2020.116321

Savenko, V. S., and Savenko, A. V. (2020). Fluorine in the surface water of bering island. *Water Resour.*, 47(4), 624–628. doi.org/doi:10.1134/S009780782004017X

Shao, S., Ma, B., Chen, Y., Zhang, W., and Wang, C. (2021). Behavior and mechanism of fluoride removal from aqueous solutions by using synthesized $CaSO_4 \cdot 2H_2O$ nanorods. *Chem. Eng. J.*, 426, 131364. doi.org/doi:10.1016/j.cej.2021.131364

Strunecka, A., and Strunecky, O. (2020). Mechanisms of fluoride toxicity: From enzymes to underlying integrative networks. *Appl. Sci.*, 10(20), 7100. doi.org/doi:10.3390/app10207100

Vithanage, M., and Bhattacharya, P. (2015). Fluoride in the environment: Sources, distribution and defluoridation. *Environ. Chem. Lett.* 13 (2), 131–147. doi:10.1007/s10311-015-0496-4

Wang, M., Zhang, L., Liu, Y., Chen, D., Liu, L., Li, C., et al. (2021). Spatial variation and fractionation of fluoride in tobacco-planted soils and leaf fluoride concentration in tobacco in Bijie City, Southwest China. *Environ. Sci. Pollut. Res.* 28 (20), 26112–26123. doi:10.1007/s11356-020-11973-9

Wang, T., Shao, Z., Yu, H., and Bah, H. (2020). Distribution of fluoride in surface water and a health risk assessment in the upper reaches of the Yongding River. *J. Geogr. Sci.* 30 (6), 908–920. doi:10.1007/s11442-020-1761-4

Wenzel, W. W., and Blum, W. E. (1992). Fluorine speciation and mobility in F-contaminated soils. *Soil Sci.* 153 (5), 357–364. doi:10.1097/00010694-199205000-00003

Wu, S., Wang, Y., Iqbal, M., Mehmood, K., Li, Y., Tang, Z., et al. (2022).Challenges of fluoride pollution in environment: Mechanisms and pathological significance of toxicity–A review. *Environ. Pollut.*, 304 119241. doi:10.1016/j.envpol.2022.119241

Xu, L. R., and Luo, K. L. (2008). Studies on mode of occurrence of fluorine in rocks. *Environ. Chem.* 27 (1), 91–95. doi:10.3321/j.issn:0254-6108.2008.01.021

Zhang, M., Hao, H., Tian, L., Wang, J., Li, Y., Sun, Y., et al. (2021). Enrichment mechanisms of gallium and indium in No. 9 coals in anjialing mine, ningwu coalfield, north China, with a preliminary discussion on their potential health risks. *Minerals*, 11(1), 64. doi:10.3390/min11010064

Zhang, Z., Li, G., Su, X., Zhuang, X., Wang, L., Fu, H., et al. (2021). Geochemical controls on the enrichment of fluoride in the mine water of the Shendong mining area, China. *Chemosphere*, 284, 131388. doi.org/10.1016/j.chemosphere.2021.131388

Zhong, J., Li, S. L., Tao, F., Yue, F., and Liu, C. Q. (2017). Sensitivity of chemical weathering and dissolved carbon dynamics to hydrological conditions in a typical karst river. *Sci. Rep.* 7 (1), 42944. doi:10.1038/SREP42944